J. Biochem. **137**, 339–347 (2005)
DOI: 10.1093/jb/mvi042

Rational Design of Dual-Functional Aptamers That Inhibit the Protease and Helicase Activities of HCV NS3

Takuya Umehara[1,2], Kotaro Fukuda[1,2], Fumiko Nishikawa[1], Michinori Kohara[3], Tsunemi Hasegawa[2] and Satoshi Nishikawa[1,*]

[1]Institute for Biological Resources and Functions, National Institute of Advanced Industrial Science and Technology (AIST), Tsukuba, Ibaraki 305-8566; [2]Department of Material and Biological Chemistry, Faculty of Science, Yamagata University, Yamagata 990-8560; and [3]Tokyo Metropolitan Institute of Medical Science, Bunkyo-ku, Tokyo 113-8613

Received November 24, 2004; accepted December 26, 2004

The hepatitis C virus (HCV) non-structural protein 3 (NS3) is a multifunctional enzyme with protease and helicase activities. It is essential for HCV proliferation and is therefore a target for anti-HCV drugs. Previously, we obtained RNA aptamers that inhibit either the protease or helicase activity of NS3. During the present study, these aptamers were used to create advanced dual-functional (ADD) aptamers that were potentially more effective inhibitors of NS3 activity. The structural domain of the helicase aptamer, #5Δ, was conjugated *via* an oligo(U) tract to the 3′-end of the dual functional aptamer NEO-III-14U or the protease aptamer G9-II. The spacer length was optimized to obtain two ADD aptamers, NEO-35-s41 and G925-s50; both were more effective inhibitors of NS3 protease/helicase activity *in vitro*, especially the helicase, with a four- to five-fold increase in inhibition compared with #5 and NEO-III-14U. Furthermore, G925-s50 effectively inhibited NS3 protease activity in living cells and HCV replication *in vitro*. Overall, we have demonstrated rational RNA aptamer design based on features of both aptamer and target molecules, as well as successfully combining aptamer function and increasing NS3 inhibition.

Key words: hepatitis C virus, NS3 helicase, NS3 protease, RNA aptamer, RNA design.

The hepatitis C virus (HCV) is the major etiological agent of non-A, non-B hepatitis, with a worldwide carriage rate of 3%. Most patients develop chronic hepatitis, and persistent infection often leads to liver cirrhosis or hepatocellular carcinoma. Recently, combination therapy with interferon and ribavirin has been found to be most effective against HCV. However, not all subtypes respond to treatment, and the drugs can cause serious side effects (*1*). The development of anti-HCV drugs with greater safety and efficacy is therefore a priority.

HCV is a single-stranded RNA virus that belongs to the *Flaviviridae* family (*2*). The ~9.6-kb genome with positive polarity encodes a precursor polyprotein (~3,010 amino acids) that is processed to structural (core protein C, and envelope glycoproteins E1 and E2) and non-structural (NS2, NS3, NS4A, NS4B, NS5A and NS5B) proteins by a host signal peptidase and two viral proteases, NS2-3 and NS3 (*3*). The NS3 protein is a multi-functional enzyme with a trypsin-like protease within the amino (N)-terminal one-third, and an NTP-dependent RNA/DNA helicase in the remaining two-thirds (*4*–*6*). It is generally accepted that the protease domain cleaves the junctions between the non-structural proteins, together with cofactor NS4A (*7*). The helicase domain unwinds the double-stranded RNA generated by the RNA-dependent RNA polymerase NS5B during genome replication (*8*, *9*). As NS3 is essential for HCV replication and proliferation, new anti-HCV drugs could potentially be directed against this protein (*10*, *11*).

Previously, we used *in vitro* selection to obtain aptamers with activity against the NS3 protease or helicase domain. The aptamers G9-I, -II and -III bound specifically to the protease domain and strongly inhibited its activity (*12*). Functional and structural analysis of the major clone aptamer G9-I allowed a minimized aptamer, ΔNEO-III, to be constructed (*13*). The three G9 aptamers were transfected into cultured cells where G9-II showed the most efficient NS3 protease-inhibitory activity (*14*, *15*). NS3 has been reported to bind preferentially to the poly(U) sequence at the (+) 3′-untranslated region (UTR) of the HCV genome (*16*, *17*). We previously tested the effect of adding an oligo(U) 14-mer to the 3′-end of ΔNEO-III (NEO-III-14U). This produced a dual-functional aptamer causing both NS3 protease and helicase inhibition (*18*). The introduction of the oligo(U) tail not only increased binding and protease inhibition, but also resulted in an additional helicase-inhibitory activity. It has also been reported that the anti-helicase aptamer "#5" binds strongly and inhibited this enzyme. Aptamer #5 comprises a 5′ single-stranded region that interacts with a cleft in the NS3 helicase domain, and a 3′-region with a conserved stem–loop structure that prevents NS3 sliding along single-stranded region of #5. It was thought that aptamer #5 traps NS3 and acts as a substitute for the HCV genomic RNA (*19*).

The aim of the present study was to develop a novel aptamer with enhanced dual-inhibitory activities for the protease and helicase functions of NS3. We rationally

*To whom correspondence should be addressed. Tel: +81-298-61-6085, Fax: +81-298-61-6159, E-mail: satoshi-nishikawa@aist.go.jp

designed advanced dual-functional (ADD) aptamers by fusing previous aptamers with known anti-protease and anti-helicase activities. The ADD aptamers were then characterized in detail using *in vitro* and cell-culture assays. This approach was successful for the rational design of aptamers with enhanced inhibitory activity toward HCV NS3.

MATERIALS AND METHODS

Design and Construction of ADD Aptamers—Two types of ADD aptamer, NEO-35-sX (introduced 8–50-mer spacer) and G925-sX (introduced 5–50-mer spacer), were designed, and their secondary structures were confirmed using the Mulfold program, which is based on the Zuker algorithm (*20*). First, we constructed longer spacer aptamers (>31-mer) using six primers; 5′-AGTAATACGACTCACTATAGGGAGAACCAGCTGGTTT-3′ and 5′-$(A)_{20}$AGGAGAGAGGAAGG-3′ were used for the NEO-35 type, 5′-AGTAATACGACTCACTATAGGGAGAATTCCGACCAGAAG-3′ and 5′-$(A)_{20}$AGAAGAGGAAGGAGAGAGGA-3′ were used for the G925 type and 5′-$(T)_{25}$GGGGACGGAGCCCTTAATG-3′ and 5′-TGGCTGCGCGTCATG-3′ were used for #5Δ. The homopolymeric tracts A_{20} or T_{25} were introduced by PCR to the 3′-end of NEO-III-14U and G9-II, or the 5′-end of #5Δ template DNA (Ex-Taq, Takara). The products were used as overlapping primers in a second PCR. Conjugated aptamers with spacers of various length (31–50-mer) were obtained randomly, and clones NEO-35-s31, -s41 and -s50, and G925-s32, -s40 and -s50, were selected. Additionally G9-II-20U was constructed by cloning the fist PCR product of G9-II type.

Aptamers with shorter spacers, NEO-35-s8 and -s15, and G925-s5 and -s15, were constructed using the same procedure with spacer-length primers; 5′-CGTCCCCAAAAAAAAAGGAGAGAGGAAAGGTAGTC-3′ (for NEO-35-s8), 5′-CGTCCCCAAAAAAAAAAAAAAAAAGGAGAGAGGAAAGGTAG-3′ (for NEO-35-s15), 5′-CTCCGTCCCCAAAAAAGGAGAGAGGAAAGGGTCCC-3′ (for G925-s5) and 5′-CGTCCCCAAAAAAAAAAAAAAAAGGAGAGAGGAAAGGGTC-3′ (for G925-s15).

RNA was transcribed from the DNA templates using an Ampliscribe T7 transcription kit (Epicentre) and purified by electrophoresis through a 7 M urea 8% polyacrylamide denaturing gel.

Expression and Purification of NS3 Protein—The expression plasmid (pT7/His-NS3) containing full-length HCV-NS3 with a His-tag fused to the N-terminus was constructed previously (*19*). *Escherichia coli* strain BL21 (DE3) was transformed with the plasmid, and recombinant NS3 was expressed and purified. *E. coli* cells were pre-cultivated in 20 ml LB medium overnight at 37°C. The culture was added to 1 liter LB medium and grown continuously at 30°C for 12 h without IPTG induction. The cells were harvested and resuspended in lysis buffer [20 mM Tris-HCl (pH 7.6), 500 mM NaCl and 5 mM imidazol]. After sonication, the lysate containing NS3 was loaded onto a Ni-NTA column (Amersham). The column was washed with PBS [20 mM PBS (pH 7.4) and 500 mM NaCl] containing 60 mM imidazol, and the bound proteins were eluted with PBS containing 100 mM and then 200 mM imidazol. The fractions containing NS3 were monitored using SDS-PAGE, pooled and then dialyzed against TNE [10 mM Tris-HCl (pH 7.6), 50 mM NaCl and 1 mM EDTA]. After microcon concentration YM-50 (Millipore), the NS3 was stored at –20°C mixed with an equal volume of glycerol (0.5× TNE and 50% glycerol).

NS3 Protease-Inhibition Assay—The protease-inhibition assay was similar to that reported previously (*12*). A dansyl-labeled synthetic peptide substrate (NS5A/5B junction sequence, 17-mer amino acid, 43 μM) was added to the premixture [50 mM Tris-HCl (pH 7.8), 5 mM $MgCl_2$, 5 mM $CaCl_2$, 10 mM DTT, 1.2 μM NS3, 13.5 μM NS4A cofactor peptide and various concentrations of aptamers]. The cleavage reaction was incubated at 25°C for 60 min, and then stopped by adding NaOH to a final concentration of 0.4 M. The reaction products were separated by reverse-phase HPLC (TSK gel ODS-120T) and the cleavage efficiency was quantitated. The assay mixture in the presence of 3 mM ATP was incubated at 37°C for 20 min and analyzed as described above.

NS3 Helicase-Inhibition Assay—The helicase-inhibition assay was carried out as reported previously (*18*). A partial duplex DNA substrate (0.13 nM), comprising a 5′-^{32}P–labeled DNA oligonucleotide (n = 30) annealed to bacteriophage M13mp18(+) ssDNA, was added to the premixture [25 mM MOPS-NaOH (pH 7.0), 2.5 mM DTT, 100 μg/ml BSA, 5 mM $MgCl_2$, 5 mM $CaCl_2$, 3 mM ATP and 100 nM NS3] and aptamers at various concentrations. The unwinding reactions were incubated at 37°C for 30 min, then stopped by adding 5 μl stop solution [0.1 M Tris-HCl (pH 7.6), 20 mM EDTA, 0.5% SDS, 0.1% nonidet P40, 0.1% bromophenol blue 0.1% xylene cyanol and 25% glycerol]. The reaction products were loaded onto an 8% native polyacrylamide gel containing 0.5× TBE, and unwinding activity was analyzed using a BAS2500 (Fuji Film).

Filter-Binding Assay—The filter-binding assay for NEO-35-s41 or G925-s50 and NS3 was performed using the same conditions as for the helicase assay, but ATP was omitted. NS3 (0.032–500 nM) was added to the reaction mixture, which contained internal labeled aptamers (5 nM). The binding reactions were incubated at 37°C for 30 min and passed through an MF™-membrane filter 0.45 μm HA (Millipore). The membrane was washed immediately with 1 ml of binding buffer without ATP, and the radioisotope activity on the membrane was counted using a BAS2500. The relative binding ratio was calculated, and the binding parameters [maximum binding (B_{max}), the equilibrium-dissociation constant (K_d) and the Hill coefficient (n_H)] were analyzed using a non-linear curve fitting the following equation: binding (%) = $100 \times B_{max}[NS3]^n/(K_d + [NS3]^n)$.

UV Cross-Linking and Electrophoretic Mobility-Shift Analysis (EMSA)—The reaction mixture used to perform UV cross-linking (10 μl) contained 0.2 μM ^{32}P-internal labeled NEO-35-s41 or G925-s50 in 25 mM MOPS-NaOH (pH 7.0), 2.5 mM DTT, 100 μg/ml BSA, 5 mM $MgCl_2$, 5 mM $CaCl_2$ and 2 μM NS3. The reaction was incubated at room temperature for 30 min and then exposed to UV irradiation (254 nM) for 30 min using a transilluminator (Mineralight UVGL-57) from a distance of 3 cm. The cross-linked samples were separated by electrophoresis through a gradient SDS polyacrylamide gel (4–20%; SuperSep, Wako) and detected using a BAS2500. The

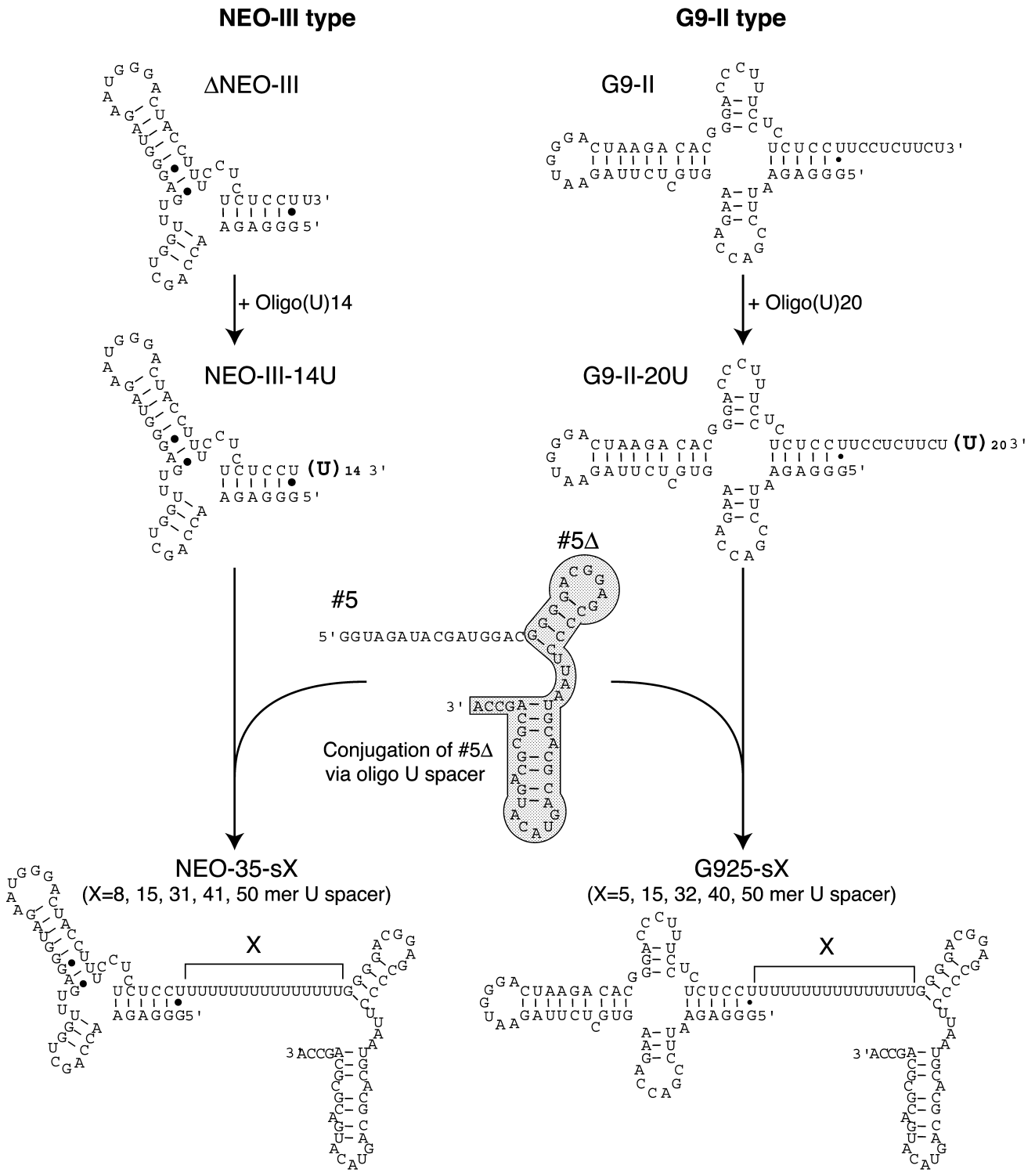

Fig. 1. **Design and construction of two types of conjugated aptamers, NEO-35-sX and G925-sX (X indicates spacer length).** They were conjugated with #5Δ (gray area), which is the structural domain of the helicase aptamer #5, at the 3′-end of the protease aptamer NEO-III-14U or G9-II *via* an oligo(U) spacer (5–50-mer). The protease aptamer, NEO-III-14U, was identified in our recent report (*18*). G9-II-20U has a 20-mer oligo(U) stretch introduced at the 3′-end of G9-II and in the middle of the G925-sX construction. Secondary structures were predicted using the Mulfold program.

molecular weight was estimated by comparison to precision-plus protein standards (Bio-Rad).

Detection of Protease-Inhibition Activity of Aptamers in HeLa Cells—The transfection of cultured cells was as reported previously, with some modifications (*14*). One day before the first transfection, a 24-well plate was seeded with 0.8×10^5 cells per well in D-MEM, 5% heat-inactivated FBS and no antibiotics, and then incubated

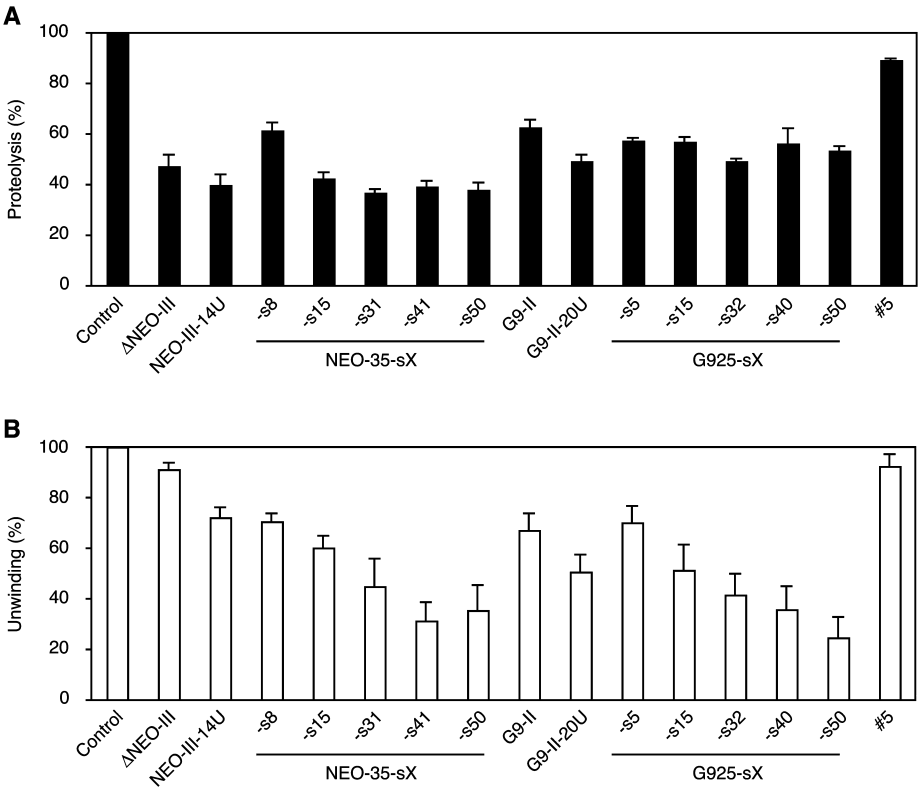

Fig. 2. **Screening of ADD aptamers by protease or helicase inhibition assays.** (A) Assay for NS3 protease inhibition. The protease-cleavage activity of 1.2 μM NS3 was evaluated in the presence of 1.2 μM aptamers. (B) Assay for NS3 helicase inhibition. The unwinding efficiency of 100 nM NS3 was evaluated in the presence of 25 nM aptamers. The control (100%) in (A) or (B) was the proteolytic or unwinding activity in the absence of RNA.

at 37°C in 5% CO_2. The cells were 70% confluent at the time of transfection. The cells were cotransfected with the NS3-expression vector pCMV/34s-2-FLAG or its mutants pCMV/34s-2-M (500 ng) and the substrate-expression vector pC5abY (25 ng) using Lipofectamine 2000 (1.5 μl; Invitrogen) according to the manufacturer's instructions. pCMV/34s-2-M was used as a negative control. After incubation for 24 h, the cells were transfected with RNA aptamers (90 pmol) using DMRIE-C (4 μl; Invitrogen). Positive and negative control cells were transfected using DMRIE-C without RNA. The cells were incubated for 1 day and harvested in passive lysis buffer (Promega). The fluorescence resonance-energy transfer (FRET) per microgram of total protein in each lysate was measured using a CytoFluor II (excitation at 430 nm; emission at 530 nm; Applied Biosystems). The relative inhibition efficiencies in HeLa cells were calculated from the FRET values using the following equation: inhibition (%) = 100 × [M – R]/[M – W]. M, R and W represent the FRET values of the negative control (NS3 mutant cell lysate), RNA aptamer-transfected cell lysate and positive control (NS3 cell lysate), respectively.

Detection of FLAG Tag Fused NS3 by Immunoblotting—Cell lysates (2 μg total protein) were separated by gradient SDS-PAGE (4–20%; Wako) and transferred to a nitrocellulose membrane (0.1 μm). The membrane was blocked with 10% skimmed milk in Tris-buffered saline with 0.1% Tween 20 (TBS-T). The primary antibody was anti-FLAG M2 monoclonal antibody (Sigma) diluted with TBS-T 10% skimmed milk (1:1,000 dilution). The membrane was washed with TBS-T, and the secondary antibody, HRP-goat anti-mouse IgG HRP (Zymed Laboratories), which was also diluted with TBS-T 10% skimmed milk, was added (1:1,000 dilution). The FLAG-tagged NS3 was detected by enhanced chemiluminescence (Amersham) and by exposure to X-ray film (Kodak).

Preparation of an In Vitro HCV-Replication System—An *in vitro* HCV-replication system was prepared from HCV replicon cells based on the procedure of Hardy *et al.* (*21*). The cells were cultivated in a T-175 bottle until they reached 90% confluence. The cells were harvested, homogenized and the ER membrane fractions (P15) were separated by centrifugation. The P15 fraction was suspended in 100 μl hypotonic buffer [10 mM Tris-HCl (pH 7.8) and 10 mM NaCl] and stored at –80°C. Assays were performed in the presence of RNA aptamers (0.1, 1 and 10 μM), and the products were separated using a 0.8% denaturing agarose gel containing 1× MOPS-EDTA and 18% formaldehyde. The gel was dried and the radioactivity incorporated into the replicated RNA was analyzed using a BAS2500.

RESULTS

Design of Advanced Dual-Functional (ADD) Aptamers—During previous studies of the human HCV NS3, we developed RNA aptamers against the protease and helicase domains: the protease inhibitors were designated G9-I, II and III (*12*), and the helicase inhibitor was designated #5 (*19*). The present study was undertaken to design ADD aptamers against both enzymatic activities of NS3 (Fig. 1). Two different 5′ components were used: ΔNEO-III, which is a minimized form of G9-I (*13*), or G9-II, which is the most efficient aptamer against NS3 protease in HeLa cells (*14*, *15*). Recently, we found that the binding and inhibitory activity of ΔNEO-III for NS3 protein was increased by conjugating an oligo(U) stretch to the 3′-end (NEO-III-14U) (*18*).

Table 1. **IC_{50} against NS3 protease or helicase.**

	Protease (1.2 μM)	Helicase (100 nM)
NEO-III-14U	0.55 ± 0.20 μM	100.0 ± 13.6 nM
NEO-35-s41	0.20 ± 0.02 μM	21.0 ± 7.92 nM
G9-II-20U	0.53 ± 0.17 μM	28.3 ± 7.25 nM
G925-s50	0.26 ± 0.11 μM	17.5 ± 5.59 nM
#5	ND	75.0 ± 35.9 nM

The protease assays were performed in the presence of 0.12, 0.24, 0.6, 1.2, 2.4, 6 and 12 μM aptamer. The helicase assays were performed in the presence of 1–1,000 nM aptamer (NEO-III-14U = 5, 25, 50, 500 and 1,000 nM; G9-II-20U = 1, 5, 10, 25, 50, 100, 500 and 1,000 nM; NEO-35-s41 and G925-s50 = 1, 5, 10, 25, 50 and 100 nM). ND, not detected.

The 3′ component was the #5 helicase aptamer. The 5′ single-stranded region of #5 could be changed to other sequences without structurally changing the 3′-domain (#5Δ) (*19*). The NS3 helicase domain preferentially binds to poly(U) or poly(U/C) tracts in the 3′-UTR of the positive strand [(+) 3′-UTR] of the HCV genome (*17*, *22*). Therefore, we inserted an oligo(U) tract between the 5′ and 3′ aptamers. We expected that the oligo(U) would function as a spacer between the two ADD aptamer domains, thereby preventing steric hindrance and maintaining the aptamer structure on both sides. Two types of ADD aptamer were constructed that simultaneously targeted the two important domains of NS3, NEO-35-sX and G925-sX, which contained spacers of varying lengths (5–50-mers) as indicated by X (Fig. 1).

Selection of the Most Efficient ADD Aptamers—NS3 protease and helicase inhibition assays were used to identify the most efficient inhibitory aptamers among our constructs. Equal amounts of each aptamer were added to a protease-inhibition assay mixture in which NS3 digested a synthetic peptide substrate. The level of inhibition by each anti-protease aptamer was increased slightly by extending an oligo(U) stretch at the 3′-end (Fig. 2A; NEO-III-14U and G9-II-20U). The inhibition efficiencies of the ADD aptamers were similar when either NEO-III-14U or G9-II-20U was used (Fig. 2A). The one exception was NEO-35-s8, with the shortest spacer, which had reduced protease inhibition efficiency. The folding of the NEO-35-s8 secondary structure for both the anti-protease and helicase aptamers was retained even with the U8 spacer. Thus, it appears that steric hindrance associated with the short spacer in NEO-35-s8 prevented it from binding to NS3. NEO-35-sXs showed greater inhibition relative to the G925-sXs aptamers under these conditions, although there seemed to be little difference between them kinetically (as described later).

The partial duplex DNA substrate was unwound by NS3 and the reaction was inhibited in the presence of ADD aptamers. The efficiency of helicase inhibition was increased by extending the length of the spacer (Fig. 2B). This result supports the idea that NS3 predominantly binds to the single-stranded region of ADD aptamers. The unwinding activity of the helicase decreased to 31% with NEO-35-s41 and to 25% with G925-s50. These two conjugated aptamers achieved the greatest inhibition among those tested. We focused next on NEO-35-s41 and G925-s50, and characterized their activity in detail.

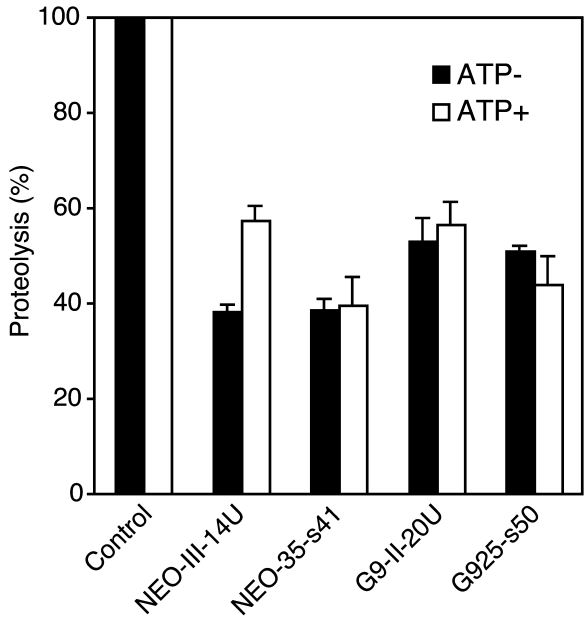

Fig. 3. **Inhibition of NS3 protease activity by aptamers in the presence or absence of ATP.** Equal amounts of each aptamer against 1.2 μM NS3 were added to the NS3 protease assay in the absence or presence of ATP (final concentration = 3 mM), and the reaction mixtures were incubated at 37°C for 20 min.

Determination of IC_{50} against NS3 Protease and Helicase Activities—The kinetics of the NEO-35-s41 and G925-s50 inhibitory activities were analyzed by comparing their NS3 protease and helicase IC_{50} values with NEO-III-14U, G9-II-20U and #5 (Table 1). The IC_{50} of the aptamers against proteolysis was determined using a proteolytic assay containing 1.2 μM NS3 in the presence of 0.12–12 μM of aptamers. The IC_{50} values of NEO-35-s41 and G925-s50 were 0.2 and 0.26 μM, respectively. These values were lower than those for NEO-III-14U (0.55 μM) and G9-II-20U (0.53 μM). The anti-helicase activities were measured using 100 nM NS3 in the presence of 1–1,000 nM aptamers. The IC_{50} values of NEO-35-s41 and G925-s50 were 21 and 17.5 nM, respectively. These values were four-fold lower than that of the anti-helicase aptamer #5 alone (75 nM). Furthermore, G9-II-20U had a lower IC_{50} value than that of the NEO-III-14U. These data imply that ADD aptamers of G9-II types are basically superior to that of NEO-III type in preventing translocation of trapped helicase without #5Δ. Thus it is considered that helicase-inhibitory efficiency is also due to a protease aptamer region of the ADD aptamer in addition to the #5Δ effect.

Inhibition of NS3 Protease Activity in the Presence of ATP—An RNA aptamer with a single-stranded region might become a substrate for NS3 helicase, and might be unwound in the presence of ATP. The protease inhibition activities of the aptamers under helicase working conditions were examined by performing the protease-inhibition assay in the presence of ATP (Fig. 3). NS3 helicase was confirmed to function under the protease-assay conditions (data not shown). Protease inhibition by G9-II-20U, NEO-35-s41 and G925-s50 was unaffected by the presence or absence of ATP. However, the inhibitory abil-

Table 2. **Summary of binding parameters.**

	Low concentration (0.032–4 nM)			High concentration (4–500 nM)		
	B_{max1} (%)	K_{d1} (nM)	n_{H1}	B_{max2} (%)	K_{d2} (nM)	n_{H2}
NEO-35-s41	17.9 ± 1.3	0.19 ± 0.16	1.2 ± 0.4	45.4 ± 1.1	6.99 ± 1.51	1.0 ± 0.1
G925-s50	12.6 ± 0.6	0.11 ± 0.06	1.9 ± 0.3	44.9 ± 1.9	12.0 ± 4.49	1.0 ± 0.2

The parameters were calculated using the non-linear least-squares curve-fitting method (±SD).

ity of NEO-III-14U decreased from 60 to 40% in the presence of ATP. This result is also reflected in the IC_{50} value of helicase (Table 1). It appears that NEO-III-14U is opened and unwound by NS3 helicase in the presence of ATP.

Determination of the Equilibrium-Dissociation Constant and Hill Coefficient—The two ADD aptamers, NEO-35-s41 and G925-s50, showed the strongest helicase-inhibition activity among the constructs tested. The reason for this was investigated by analyzing the binding of NEO-35-s41 and G925-s50 to NS3 at different concentrations under the helicase-assay conditions without ATP. As a result, we observed two plateaus in the binding curves. The first appeared at 1–4 nM of NS3 and ~10–20% of ADD aptamers bound to NS3 (Fig. 4A). The second plateau appeared at over 100 nM NS3, where ~40% of the maximum binding activity was observed (Fig. 4B). The data were fitted by the non-linear least-squares method (see Materials and Methods) under low and high NS3 concentrations (Table 2). This indicated that there are two binding states between ADD aptamers and NS3 that are affected by its concentration: positive cooperativity ($n > 1$) occurs at low concentrations (0.032–4 nM) of NS3 and non-cooperativity ($n = 1$) occurs at high concentrations (4–500 nM) of NS3. This indicates that NS3 can bind more easily to ADD aptamers at low concentrations than at high concentrations.

Electrophoretic Mobility-Shift Analysis (EMSA) by UV Cross-Linking—The complexes formed between ADD aptamers and NS3 were examined directly by performing

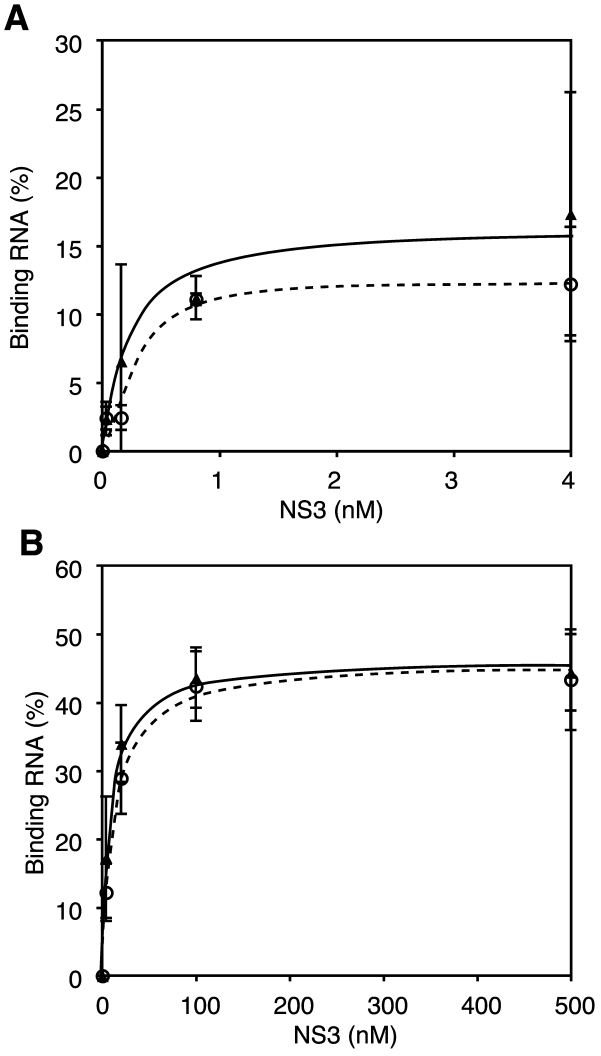

Fig. 4. **Saturated binding curves of NS3 and NEO-35-s41 (filled triangles) or G925-s50 (open circles) were fitted by the non-linear least-squares method.** (A) represents low concentrations of NS3 (0–4 nM), whereas (B) indicates high concentrations (4–500 nM).

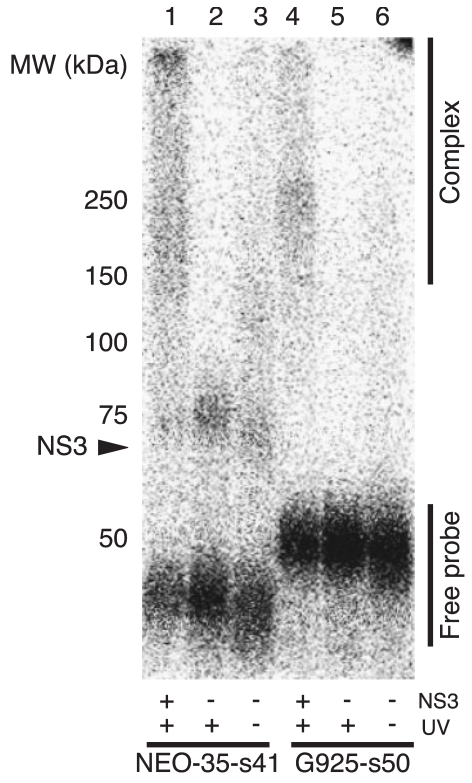

Fig. 5. **EMSA employing UV cross-linking and SDS-PAGE.** The complexes formed between NS3 and conjugated aptamers (internal labeling) were cross-linked by UV irradiation. The samples were then loaded onto a 4–20% gradient SDS polyacrylamide gel. Lanes 1 and 4 were UV irradiated within NS3. Lanes 2 and 5 were UV irradiated without NS3. Lanes 3 and 6 lacked UV exposure and NS3. The molecular sizes of the complexes were estimated by comparison with prestained markers.

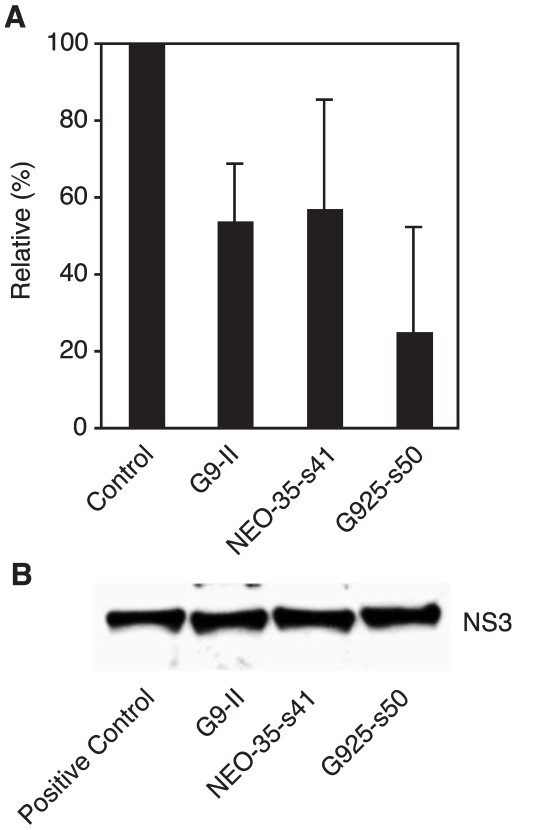

Fig. 6. **(A) NS3 protease-inhibition assay in HeLa cells.** The inhibition efficiency was analyzed by FRET of C5abY substrate protein. **(B) The expression level of FLAG fused NS3 in the cell lysate was assessed by immunoblotting.**

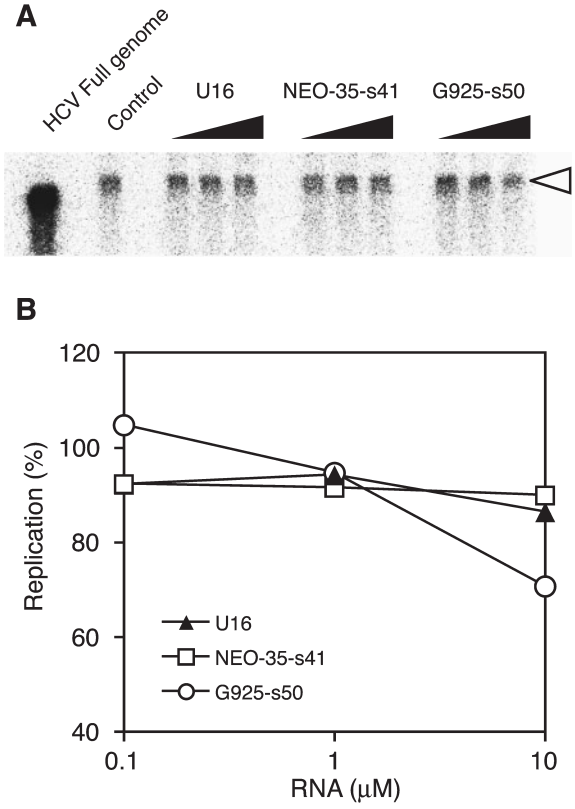

Fig. 7. **HCV genome-replication assay of NEO-35-s41 and G925-s50 using an *in vitro* HCV-replication system.** (A) The reaction mixtures were separated in a 0.8% denaturing agarose gel containing 1× MOPS-EDTA buffer. The open arrowhead indicates the replicated replicon genome. (B) The intensities of the bands from the replicated RNA genome were quantitated using a BAS2500.

EMSA using ^{32}P-labeled aptamers (Fig. 5). The complexes formed by either NEO-35-s41 or G925-s50 with NS3 after UV cross-linking were detected as broad bands with a molecular mass over 150 kDa (lanes 1 and 4). The NEO-35-s41 complex was observed as a band at ~150–250 kDa and also remained within the sample well (lane 1). Interestingly, an 80-kDa band was also observed in the absence of NS3 (lanes 2 and 3), suggesting that NEO-35-s41 forms a dimer. Thus, dimerized NEO-35-s41 must form a macromolecule by binding to several NS3 molecules. In contrast, the size of the complex of G925-s50 and NS3 was ~250 kDa (lane 4). As the molecular masses of G925-s50 and NS3 are ~52 and 70 kDa, respectively, one G925-s50 aptamer could capture three NS3 molecules.

Inhibition of NS3 Protease Activity in HeLa Cell by ADD Aptamers—The inhibitory activity of aptamers within living cells was investigated by transfecting HeLa cells with various different aptamers (90 pmol). The HeLa cells were transiently expressing NS3 and a substrate protein that comprised two types of GFP derivatives connected by a NS3 cleavage site (C5abY) (*14*). This system allows the inhibition of NS3 protease activity to be detected easily by FRET. NEO-35-s41 and G925-s50 caused 45 and 75% inhibition of NS3 proteolysis, respectively (Fig. 6A). NEO-35-s41 achieved the same level of inhibition as G9-II, but G925-s50 was most effective among these three aptamers. The level of NS3 expression was detected by immunoblotting and was not reduced by transfection with aptamers (Fig. 6B). We, therefore, propose that the inhibitory effect of the aptamers is specific for the protease activity of NS3.

Inhibition of HCV Replication Using an In Vitro HCV Replicon Genome-Replication System—We evaluated the ability of NEO-35-s41 and G925-s50 to inhibit HCV replication in an *in vitro* system. The aptamers were added at concentrations of 0.1, 1 and 10 μM (Fig. 7) to a system containing the components of HCV replication, that is, the replicase (non–structural proteins complex) and replicon (genome). The genome can be copied by the replicase in this system (*21*). Thus, this technique is appropriate for the rapid *in vitro* evaluation of the efficiency of HCV-replication inhibitors. The replicated band was detected in the replicon cell lysate but not in the Huh-7 lysate (data not shown). U_{16} (negative control) and NEO-35-s41 did not affect the replication reaction; however, G925-s50 caused moderate inhibition (30%). Our data, therefore, suggest that G925-s50 inhibits the NS3 helicase stage of the replication process.

DISCUSSION

In this study, novel RNA aptamers were designed to attack two important domains of the HCV NS3 protein (ADD aptamer; Fig. 1) simultaneously. As expected, all of

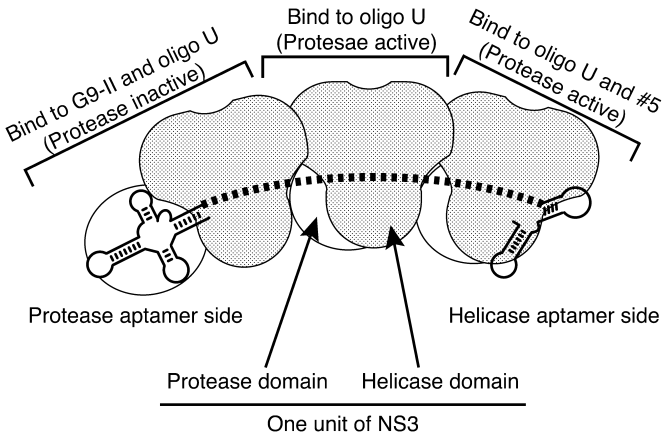

Fig. 8. **Binding model of G925-s50 with NS3. G925-s50 probably binds to three NS3 molecules.** One of the three NS3s binds to the protease aptamer side and inhibits both the protease and helicase activities, while the other two NS3 molecules bind to the central oligo(U) region and the helicase aptamer region to inhibit the helicase activity.

the aptamers had a dual-inhibitory function as a result of conjugating oligo(U) and #5Δ to the NEO-III-14U obtained previously (Fig. 2). Any RNA with a single-stranded region could, in theory, provide a substrate for the NS3 helicase; however, the ADD aptamers did not, and they strongly inhibited both NS3 enzymatic activities (Fig. 3).

Among the constructs tested, NEO-35-s41 and G925-s50 inhibited both the protease and helicase activities of NS3 most effectively. The length of the spacer incorporated into the ADD aptamer affected the efficiency of the inhibition. During HCV replication, the NS3 protein binds to the 3′-UTR, (the site for replication initiation) and unwinds the replicated double-stranded RNA in the 3′ to 5′ direction (*17*). The length of the poly(U/C) tract in the (+) 3′-UTR is important for optimal interaction with NS3; at least 50–62 nucleotides are required for effective replication (*23*). Therefore, we propose that an oligo(U) spacer of 41–50 residues provides an optimal interaction with NS3, enhancing the efficiency of the inhibition by both the anti-protease and anti-helicase aptamers. Furthermore, we reported previously that a variable region in the (+) 3′-UTR regulates the translocation of NS3 helicase, and that the higher-order structure correlates with this regulation (*19*). Accordingly, the slight difference in the efficiency of helicase inhibition by NEO-35-s41 and G925-s50 might be due to the stability of the anti-protease aptamer structure.

The binding of the ADD aptamers NEO-35-s41 and G925-s50 to NS3 was analyzed using a filter-binding assay and EMSA. It appeared that several NS3 molecules efficiently bound to each ADD aptamer. Interestingly, this binding cooperativity varied according to the concentration of NS3: we detected positive cooperativity at low NS3 concentrations and non-cooperativity at high concentrations (Fig. 4 and Table 2). Monomeric NS3 forms dimers or tetramers depending on its concentration (*24*, *25*). The observed change in cooperativity is likely to correspond to the point at which oligomer-formation occurs. Furthermore, EMSA reveals the molecular size of the complex directly (Fig. 5). We could not identify the ratio of NEO-35-s41 to NS3 within this complex, because the NEO-35-s41 dimerized and could form macromolecules with an oligomeric NS3 protein. However, we could clearly identify a 1:3 molar ratio of molecules in the complex between G925-s50 and NS3 (Fig. 8). It is likely that ADD aptamers bind not only to NS3 monomers and dimers, but also to NS3 tetramers. However, as the EMSA was performed under denaturing conditions, only NS3 that was strongly bound to the ADD aptamer would be detected. These data indicate that both NEO-35-s41 and G925-s50 interact strongly with several NS3 molecules, regardless of oligomer formation, and this inhibits helicase and protease activities. Moreover, our results are consistent with the difference observed in inhibition efficiency between protease and helicase activities. We propose that protease inhibition requires a 1:1 stoichiometry between the ADD anti-protease aptamer and NS3, whereas helicase inhibition occurs when several NS3 molecules interact in the region of the oligo(U) spacer and anti-helicase aptamer. G925-s50 appears to trap at least three NS3 molecules and strongly inhibits the sliding of NS3 helicase (Fig. 8).

Two ADD aptamers, NEO-35-s41 and G925-s50, were evaluated as HCV NS3 inhibitors under similar conditions to those found *in vivo* using a protease assay in living cells and an HCV *in vitro* genome-replication system (Figs. 6 and 7). The results of both assays indicated that the aptamer G925-s50 is a more effective inhibitor than NEO35-s41. The efficiency of the two aptamers was similar in the protease inhibition assay. When the inhibitors are applied to living cells, the instability of the NEO-35-s41 structure might be magnified, because the ΔNEO-III aptamer requires more calcium ions than magnesium for the optimal inhibition of NS3 protease, despite the fact that G9-II does not (*13*). Generally, the concentrations of calcium ions are lower than those of magnesium ions in living cells. Furthermore, calcium ions were not added to the *in vitro* HCV genome-replication system, as this might inhibit the effectiveness of NEO-35-s41. Therefore, we suggest that G925-s50 offers advantages in terms of both NS3 protease and helicase inhibition, and should be the candidate of choice for use as an anti-HCV drug. We rationally designed novel ADD RNA aptamers by conjugating two aptamers and adjusting their distance. Additional research on the conjugation of other aptamers will enlarge the field of aptamer application.

We thank Dr. T. Watanabe and Dr. M. Shuda (Tokyo Metropolitan Institute of Medical Science, Japan) for helpful discussions.

REFERENCES

1. Rosenberg, S. (2001) Recent advances in the molecular biology of hepatitis C virus. *J. Mol. Biol.* **313**, 451–464
2. Choo, Q.L., Richman, K.H., Han, J.H., Berger, K., Lee, C., Dong, C., Gallegos, C., Coit, D., Medina-Selby, A., Barr, P.J., Weiner, A.J., Bradley, D.W., Kuo, G., and Houghton, M. (1991) Genetic organization and diversity of the hepatitis C virus. *Proc. Natl. Acad. Sci. USA* **88**, 2451–2455
3. Major, M.E. and Feinstone S.M. (1997) The molecular virology of hepatitis C. *Hepatology* **25**, 1527–1538

4. Grakoui, A., McCourt, D.W., Wychowski, C., Feinstone, S.M., and Rice, C.M. (1993) Characterization of the hepatitis C virus-encoded serine proteinase: determination of proteinase-dependent polyprotein cleavage sites. *J. Virol.* **67**, 2832–2843
5. Tomei, L., Failla, C., Santolini, E., De Francesco, R., and La Monica, N. (1993) NS3 is a serine protease required for processing of hepatitis C virus polyprotein. *J. Virol.* **67**, 4017–4026
6. Kim, D.W., Gwack, Y., Han, J.H., and Choe, J. (1995) C-terminal domain of the hepatitis C virus NS3 protein contains an RNA helicase activity. *Biochem. Biophys. Res. Commun.* **215**, 160–166
7. Failla, C., Tomei, L., and De Francesco, R. (1994) Both NS3 and NS4A are required for proteolytic processing of hepatitis C virus nonstructural proteins. *J. Virol.* **68**, 3753–3760
8. Behrens, S.E., Tomei, L., and De Francesco, R. (1996) Identification and properties of the RNA-dependent RNA polymerase of hepatitis C virus. *EMBO J.* **15**, 12–22
9. De Francesco, R. and Steinkuhler, C. (2000) Structure and function of the hepatitis C virus NS3-NS4A serine proteinase. *Curr. Top. Microbiol. Immunol.* **242**, 149–169
10. Dymock, B.W. and Jones, P.S., and Wilson, F.X. (2000) Novel approaches to the treatment of hepatitis C virus infection. *Antivir. Chem. Chemother.* **11**, 79–96
11. Bianchi, E. and Pessi, A. (2002) Inhibiting viral proteases: challenges and opportunities. *Biopolymers* **66**, 101–114
12. Fukuda, K., Vishnuvardhan, D., Sekiya, S., Hwang, J., Kakiuchi, N., Taira, K., Shimotohno, K., Kumar, P.K.R., and Nishikawa, S. (2000) Isolation and characterization of RNA aptamers specific for the hepatitis C virus nonstructural protein 3 protease. *Eur. J. Biochem.* **267**, 3685–3694
13. Sekiya, S., Nishikawa, F., Fukuda, K., and Nishikawa, S. (2003) Structure/function analysis of an RNA aptamer for hepatitis C virus NS3 protease. *J. Biochem.* **133**, 351–359
14. Kakiuchi, N., Fukuda, K., Nishikawa, F., Nishikawa, S., and Shimotohno, K. (2003) Inhibition of hepatitis C virus serine protease in living cells by RNA aptamers detected using fluorescent protein substrates. *Comb. Chem. High Throughput Screen.* **6**, 155–160
15. Nishikawa, F., Kakiuchi, N., Funaji, K., Fukuda, K., Sekiya, S., and Nishikawa, S. (2003) Inhibition of HCV NS3 protease by RNA aptamers in cells. *Nucleic Acids Res.* **31**, 1935–1943
16. Kanai, A., Tanabe, K., and Kohara, M. (1995) Poly(U) binding activity of hepatitis C virus NS3 protein, a putative RNA helicase. *FEBS Lett.* **376**, 221–224
17. Banerjee, R. and Dasgupta, A. (2001) Specific interaction of hepatitis C virus protease/helicase NS3 with the 3′-terminal sequences of viral positive- and negative-strand RNA. *J. Virol.* **75**, 1708–1721
18. Fukuda, K., Umehara, T., Sekiya, S., Kikuchi, K., Hasegawa, T., and Nishikawa, S. (2004) An RNA ligand inhibits hepatitis C virus NS3 protease and helicase activities. *Biochem. Biophys. Res. Commun.* **325**, 670–675
19. Nishikawa, F., Funaji. K., Fukuda, K., and Nishikawa, S. (2004) *In vitro* selection of RNA aptamer against the HCV NS3 helicase domain. *Oligonucleotides* **14**, 114–129
20. Zuker, M. (1989) Computer prediction of RNA structure. *Methods Enzymol.* **180**, 262–288
21. Hardy, R.W., Marcotrigiano J., Blight, K.J., Majors, J.E., and Rice, C.M. (2003) Hepatitis C virus RNA synthesis in a cell-free system isolated from replicon-containing hepatoma cells. *J. Virol.* **77**, 2029–2037
22. Friebe, P., and Bartenschlager, R. (2002) Genetic analysis of sequences in the 3′ nontranslated region of hepatitis C virus that are important for RNA replication. *J. Virol.* **76**, 5326–5338
23. Yi, M. and Lemon, S.M. (2003) 3′ nontranslated RNA signals required for replication of hepatitis C virus RNA. *J. Virol.* **77**, 3557–3568
24. Levin, M.K. and Patel, S.S. (1999) The helicase from hepatitis C virus is active as an oligomer. *J. Biol. Chem.* **274**, 31839–31846
25. Locatelli, G.A., Spadari, S., and Maga, G. (2002) Hepatitis C virus NS3 ATPase/helicase: an ATP switch regulates the cooperativity among the different substrate binding sites. *Biochemistry* **41**, 10332–10342